The Role of New Technologies in Defining a Manufacturing Process for PPAR alpha Agonist LY518674

ARTICLE *in* ORGANIC PROCESS RESEARCH & DEVELOPMENT · MARCH 2009

Impact Factor: 2.53 · DOI: 10.1021/op8002486

Organic Process Research & Development **2009,** *13,* 131–143

Full Papers

The Role of New Technologies in Defining a Manufacturing Process for PPARα Agonist LY518674†

Mark D. Argentine, Timothy M. Braden, Jeffrey Czarnik, Edward W. Conder, Steven E. Dunlap, Jared W. Fennell, Mark A. LaPack, Roger R. Rothhaar, R. Brian Scherer, Christopher R. Schmid,‡ Jeffrey T. Vicenzi, Jeffrey G. Wei, and John A. Werner*

Chemical Product Research and Development, Lilly Research Laboratories, A Division of Eli Lilly and Company, Lilly Corporate Center, Indianapolis, Indiana 46285, U.S.A.

Robert T. Roginski

Eigenvector Research, Inc., 3905 West Eaglerock Drive, Wenatchee, Washington 98801, U.S.A.

Abstract:

The impact of several new technologies on the development of a manufacturing process for LY518674 is described. Extensive use of process analytical technology (PAT) throughout development, both at laboratory and pilot-plant scale, enabled data-rich experiments, shortened development cycle times, and obviated the requirement of PAT for process control at larger scale. In situ ReactIR was used to develop a kinetic model for a one-pot preparation of a semicarbazide intermediate. Parallel crystallizers fitted with online focused-beam reflectance measurement (FBRM) and particle vision and measurement (PVM) probes were used in the development of several challenging crystallization processes. Application of the process knowledge afforded by these technologies, combined with the principles of Quality by Design, resulted in excellent purity control throughout the four-step process. A single, 5-min, MS-friendly method capable of separating over 30 components was developed using a combination of chromatography modeling software, sub-2 μm column technology, and higher-pressure LC equipment. The method was used across all four processing steps, greatly facilitating impurity tracking, and reducing assay time and solvent use by 85% and 93%, respectively.

Introduction

New technologies are playing an increasingly important role in the development of chemical processes within the pharmaceutical industry. Process analytical technology, automation, parallel reactions, continuous processing, and fast, high-resolution assays are enabling data-rich experiments that enhance process knowledge in shorter development time frames. Combined with the principles of Quality by Design, this knowledge results in more robust manufacturing processes, thereby ensuring the patient receives medicines of the highest quality.[1,2]

This contribution highlights the impact of several technologies on both productivity and process understanding during the development of a manufacturing process for PPARα agonist LY518674 (**1**). Process analytical technology (PAT) was used extensively, both in the laboratory and in the pilot plant, with the objective of designing quality into each processing step through increased process understanding.[3] The desired result is a robust process that consistently delivers active pharmaceutical ingredient (API) with the appropriate quality attributes[4] without the requirement of PAT for process control in manufacturing.

Applications of the technologies listed below are exemplified in the present paper, which focuses on development of process and impurity control strategies to enable the preparation of API for registration-phase studies.

- ultra high-pressure chromatography and sub-2 μm column technology for rapid assays and impurity tracking.
- chromatography modeling software for method optimization in the separation of more than 30 components.
- in situ ReactIR for kinetic modeling of a KOCN reaction profile.
- online vapor-phase MS for monitoring residual oxalyl chloride during a pilot plant distillation operation.
- parallel crystallizers fitted with in situ focused-beam reflectance measurement (FBRM) and particle vision and measurement (PVM) probes for expedited crystallization development.

† This paper is dedicated to the memory of our colleague, Dr. Christopher Schmid (1959−2007). His integrity, passion for science, and faith in God were an inspiration to us all.

* To whom correspondence should be addressed. Telephone: (317) 276-9385. E-mail: jwerner@lilly.com.

‡ Chris Schmid passed away 26 December 2007.

(1) *Pharmaceutical cGMPs for the 21st Century - A Risk-Based Approach.* Final Report. Department of Health and Human Services, U.S. Food and Drug Administration: Washington, D.C., Fall (September) 2004; see http://www.fda.gov/cder/gmp/gmp2004/GMP_finalreport2004.htm.

(2) See *ICH Guidelines Q8, Annex to Q8, and Q9*; Available online at: http://www.ich.org/cache/compo/363-272-1.html.

(3) *Guidance for Industry: PAT - A Framework for Innovative Pharmaceutical Development, Manufacturing, and Quality Assurance*. Department of Health and Human Services, U.S. Food and Drug Administration: Washington, D.C., September 2005. See http://www.fda.gov/cder/guidance/6419fnl.pdf.

(4) Ganzer, W. P., Materna, J. A., Mitchell, M. B., Wall, L. K. Current Thoughts on Critical Process Parameters and API Synthesis. *Pharmaceutical Technology*; July 2, 2005. Available online at http://pharmtech.findpharma.com/pharmtech/content/printContentPopup.jsp?id=170114.

10.1021/op8002486 CCC: $40.75
Published on Web 02/03/2009

LY518674 (**1**),[5] is a highly potent and selective agonist of peroxisome proliferator-activated receptor alpha (PPARα).[6,7] It was recently evaluated in phase II clinical studies in patients with dyslipidemia and hypercholesterolemia at doses of 10−100 μg/day.[8]

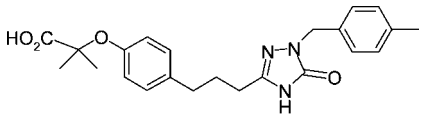

LY518674 (**1**)

The starting point for our research was the route selected for further development by Dr. Christopher Schmid and his colleagues (Scheme 1).[9] The convergent synthesis involves the coupling of semicarbazide **3** and carboxylic acid **5** to give acylsemicarbazide **7**. Semicarbazide **3** was prepared regiospecifically in three steps from commercially available 4-methylbenzaldehyde in 69% overall yield. Carboxylic acid **5** was obtained in one step by monoalkylation of the dianion of 4-hydroxyphenylbutyric acid (**4**).[10] Treatment of acylsemicarbazide **7** with 10-camphorsulfonic acid (CSA) afforded triazolone **8** via an acid-mediated cyclization. Purification by treatment with Amberlyst 15, followed by crystallization, afforded **8** in 50−55% yield from **5**. Hydrolysis of the ester with aqueous base completed the synthesis of LY518674 (**1**) in 36% overall yield from **2**.

Scheme 1. **Initial route selected for development**[a]

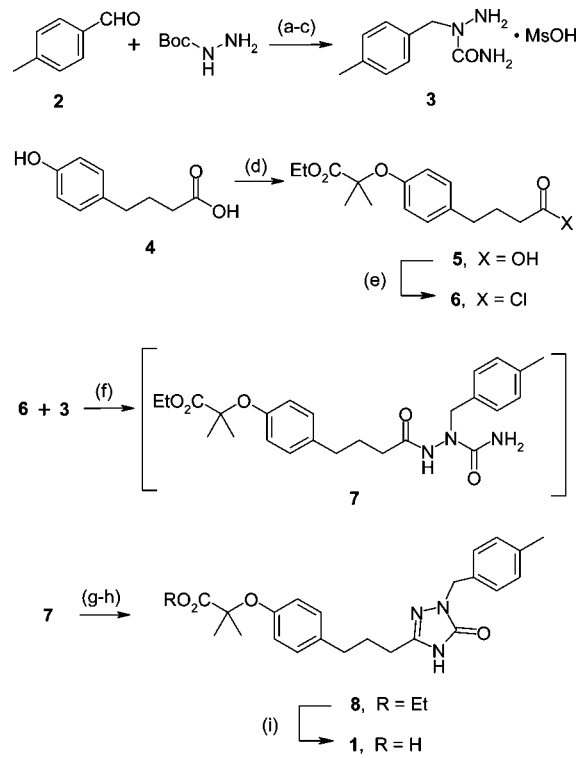

[a] Reagents and conditions: (a) 50 psig H_2, 5% Pt/C, THF, 50 °C, 8 h, 85%; (b) TMS-NCO (1.5 equiv), IPA, rt, 16 h, 86%; (c) MsOH (1.1 equiv), CH_2Cl_2, reflux, 16 h, 95%; (d) NaOEt (2 equiv), EtOH, EtOAc, reflux, 0.5 h; add **4**, reflux 0.5 h; add $EtO_2CCBr(CH_3)_2$ (3 equiv), reflux 1 h; add NaOEt (1 equiv) over 1 h, reflux 0.5 h; acidify with H_3PO_4, remove EtOH and crystallize, 95%; (e) oxalyl chloride (1.15 equiv), DMF (0.05 equiv), EtOAc, rt, 30 min; (f) pyridine (2.3 equiv), EtOAc, 0 °C; (g) CSA (1.1 equiv), EtOAc, reflux, 6 h; (h) Amberlyst 15, EtOAc, reflux, 1 h; MTBE (recrystallization), 50−55% overall from **5**; (i) NaOH, H_2O, toluene, rt, 4 h; HCl, EtOAc, distill; crystallize from EtOAc, 95%.

Results and Discussion

Development of a robust impurity control strategy for the active pharmaceutical ingredient (API) was one of our primary objectives.[11] Characterization of API from earlier campaigns using a combination of HPLC, LC−MS, and LC−NMR resulted in the identification of compounds **9**−**14** (Scheme 2), which were then synthesized (see Supporting Information for experimental procedures). Their low rejection in the final crystallization step required us to understand their origin in order to reliably control them at levels below 0.1%.[12]

A single, fast HPLC method was desired to track the formation and fate of starting materials, intermediates, and process-related impurities. With a single method, tracking of impurities across multiple steps is simplified, easily monitoring impurities being formed or removed as the synthesis progresses. Use of HPLC mobile-phase systems compatible with both UV and MS detection was also desired for efficient, information-rich data generation. However, this goal is often challenging based upon the number of components to separate and the potentially wide range of polarities associated with them.

(5) (a) Wang, X.; Barr, R. J.; Bean, J. S.; Kauffman, R. F.; Mayhugh, D. R.; Montrose-Rafizadeh, C.; Renner, J.; Saeed, A.; Singh, J.; Zink, R. W.; Mantlo, N. B. *Abstracts of Papers*, MEDI-363; 224th ACS National Meeting, Boston, MA, U.S.A., August 18−22, 2002, American Chemical Society: Washington, D.C., 2002. (b) Mantlo, N. B.; Collado Cano, I.; Dominianni, S. J.; Etgen, G. J., Jr.; Garcia-Paredes, C.; Johnston, R. D.; Letourneau, M. E.; Martinelli, M. J.; Mayhugh, D. R.; Saeed, A.; Thompson, R. C.; Wang, X.; Coffey, D. S.; Schmid, C. R.; Vicenzi, J. T.; Xu, Y. Peroxisome Proliferator Activated Receptor Alpha Agonists. WO/2002/0238553, 2002. (c) For a discussion of the SAR, see: Xu, Y.; Mayhugh, D.; Saeed, A.; Wang, X.; Thompson, R. C.; Dominianni, S. J.; Kauffman, R. F.; Singh, J.; Bean, J. S.; Bensch, W. R.; Barr, R. J.; Osborne, J.; Montrose-Rafizadeh, C.; Zink, R. W.; Yumibe, N. P.; Huang, N.; Luffer-Atlas, D.; Rungta, D.; Maise, D. E.; Mantlo, N. B. *J. Med. Chem.* **2003**, *46*, 5121–5124. (d) For a discussion of the pharmacology, see: Singh, J. P.; Kauffman, R.; Bensch, W.; Wang, G.; McClelland, P.; Bean, J.; Montrose, C.; Mantlo, N.; Wagle, A. *Mol. Pharmacol.* **2005**, *68*, 763–768.

(6) "Peroxisome proliferator-activated receptors (PPARs) are members of the nuclear hormone receptor superfamily of ligand-dependent transcription factors. [They] participate in a broad spectrum of biological processes, including cell differentiation, energy balance, lipid metabolism, insulin sensitivity, bone formation, inflammation and tissue remodeling." Quote taken from: Guan, Y.; Zhang, Y.; Breyer, M. D. *Drug News Perspect.* **2002**, *15*, 147–154.

(7) For a recent review of PPARα in the pathogenesis of metabolic syndrome in relation to diabetes and atherosclerosis, see: (a) Staels, B. *Ther. Res.* **2006**, *27*, 1347–1358. See the following for specific therapeutic areas: (b) Human metabolic syndrome: Azhar, S.; Kelley, G. *Future Lipidol.* **2007**, *2*, 31–53. (c) Immunosuppressive agents: Cunard, R. *Curr. Opin. Invest. Drugs* **2005**, *6*, 467–472. (d) Diabetic nephropathy: Varghese, Z.; Moorhead, J. F.; Ruan, X. Z. *Kidney Int.* **2006**, *69*, 1490–1491.

(8) Nissen, S. E.; Nicholls, S. J.; Wolski, K.; Howey, D. C.; McErlean, E.; Wang, M.-D.; Gomez, E. V.; Russo, J. M. *J. Am. Med. Assoc.* **2007**, *297*, 1362–1373.

(9) Braden, T. M.; Coffey, D. S.; Doecke, C. W.; LeTourneau, M. E.; Martinelli, M. J.; Meyer, C. L.; Miller, R. D.; Pawlak, J. M.; Pedersen, S. W.; Schmid, C. R.; Shaw, B. W.; Staszak, M. A.; Vicenzi, J. T. *Org. Process Res. Dev.* **2007**, *11*, 431–440.

(10) For the preparation of **4**, see: (a) Schmid, C. R.; Beck, C. A.; Cronin, J. S.; Staszak, M. A. *Org. Process Res. Dev.* **2004**, *8*, 670−673. For an alternative approach using HBr, see: (b) Delhaye, L.; Diker, K.; Donck, T.; Merschaert, A. *Green Chem.* **2006**, *8*, 181–182.

(11) A brief summary of this work has been disclosed previously: Fennell, J. W.; Dunlap, S. E.; Metzler, R.; Vicenzi, J. T.; Werner, J. A. *Abstracts of Papers*; ORGN-009. 234th ACS National Meeting, Boston, MA, United States, August 19−23, 2007; American Chemical Society: Washington, D.C., 2007.

(12) API impurity levels were as follows: **9** (0.26%), **10** (0.05%) **11** (0.18%) **12** (0.18%), **13** (0.10), and **14** (0.12%). The HPLC method for this analysis is described in the Supporting Information.

Scheme 2. **Impurities found in early lots of 1**

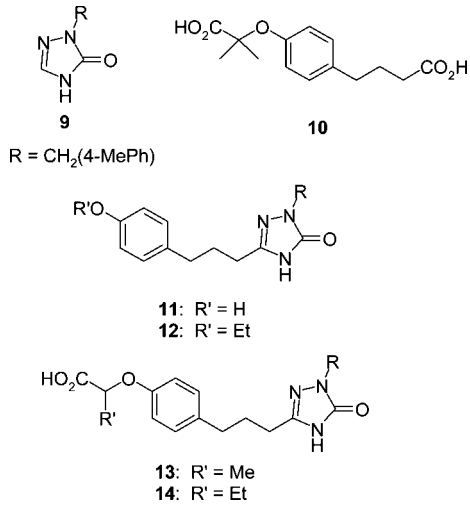

Application of Advanced HPLC Technology for "Fast-Assay" Development. The initial analytical method was developed on a Zorbax RX-C18 column (4.6 mm × 250 mm, 5 μm particles), aided dramatically by availability of pure samples for most components along with a chromatographic software modeling tool (DryLab 2000)[13] to rapidly optimize the separation. However, each sample required 30 min per injection at a flow rate of 1.5 mL/min, plus time for equilibration. The method conditions were later adapted to a Zorbax SB-C18 phase, a similar C-18 phase that offered broader availability of particle sizes and column dimensions for future efficiency gains. Use of the Zorbax SB-C18 4.6 mm × 250 mm column with 5 μm particles afforded similar separation, although it still required over 20 min per injection despite an increase in flow rate to 2 mL/min.

Advances in the use of smaller-particle columns, as well as higher-pressure LC instrumentation, were explored to further improve analysis time without reducing separation efficiency. Two parallel paths were pursued for evaluation of smaller-particle columns: chromatographic modeling and column scaling.

DryLab separation modeling software was applied successfully to the sub-2 μm column format to simplify the daunting task of direct method development and optimization for a mixture with over 30 components consisting of starting materials, intermediates, and process-related impurities. Optimization was performed using data from two linear gradients (10 and 30 min) at 40 °C. As seen in Figure 1, the predicted and actual separations compare quite well.[14] A labeled chromatogram indicating the identity of each component is available in the Supporting Information.

Scaling from the original 4.6 mm × 250 mm, 5 μm column to smaller-particle columns was performed by mathematically scaling the gradient based upon the changes in flow rate and column length to maintain comparable linear velocity and column-volume gradient programs. Scaling to the 3.5 μm column was performed with a drop in flow rate to maintain an operating pressure comparable to that of the 5 μm column. Scaling to the 1.8 μm column also required a reduced flow rate but took advantage of the higher operating pressure available with the higher-pressure LC system employed for the analysis (maximum pressure of 600 bar). The impact of high-efficiency sub-2 μm column technology is illustrated in Figure 2, comparing the chromatographic separation obtained initially by using the 5 μm particle-size column to separations using the 3.5 and 1.8 μm particle-size columns. As appropriate, gradients and injection volumes were scaled for equivalent column volumes and load capacities. Reduction in run time by approximately one-third was easily achieved while maintaining, and often enhancing, component separations.

The speed of analysis was further enhanced by mapping the separation to an ACQUITY BEH-C18 column (1.7 μm packing) that could operate at even higher pressures (~1000 bar) using the Waters ACQUITY UPLC. As shown in Figure 3, acceptable separation was achieved in less than 10 min with a 150 mm column. In fact, a 5-min analysis time could be achieved without a dramatic loss in resolution by reducing the column length to

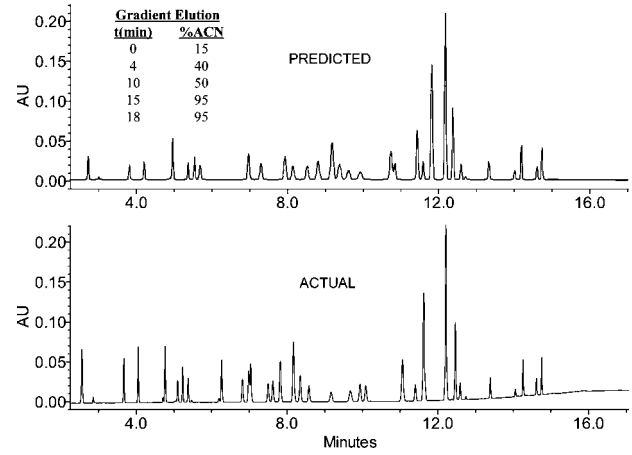

Figure 1. **Comparison of the optimized DryLab prediction (top) with the actual separation (bottom) of a 36-component mixture on a Zorbax SB-C18 (2.1 mm × 150 mm, 1.8 μm) at 40 °C and 0.4 mL/min.**

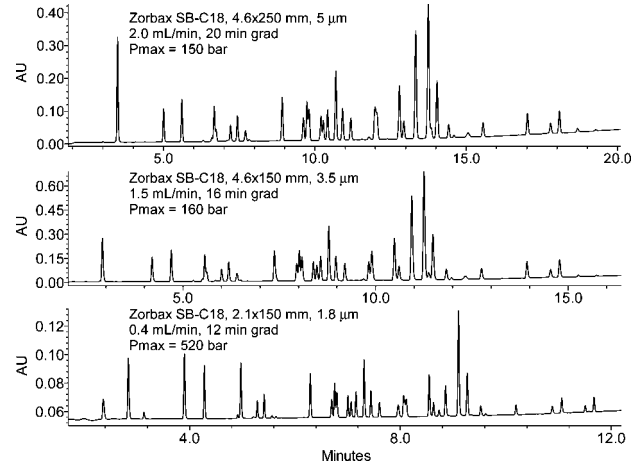

Figure 2. **Comparison of separation performance with three different particle-size columns on an Agilent 1200 SL system.**

(13) Molnar Institut für angewandte Chromatographie, Schneeglöckchenstrasse 47, D-10407 Berlin, Germany; http://www.molnar-institut.com/cd/indexe.htm.

(14) Details of this work have recently been reported: Scherer, R. B.; Argentine, M. D.; Werner, J. A. *Utilization of Technological Advances in HPLC to Improve Separations and Cycle Times*, Abstract #551; HPLC 2006, San Francisco, CA, 2006.

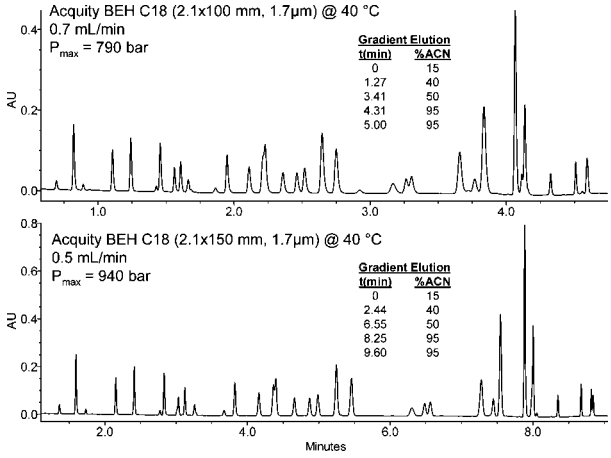

Figure 3. **Optimized separation: comparison of 100 mm (top) and 150 mm (bottom) ACQUITY BEH-C18 columns (1.7 μm particle size, 2.1 mm i.d.) on a Waters ACQUITY UPLC system.**

100 mm, which also allowed an increase in flow rate. The result was a single, fast, MS-friendly method for reaction monitoring and impurity tracking with a greater than 6-fold improvement in assay time versus the initial method (see Supporting Information for method conditions).

Fast LC assays have a dramatic impact on both productivity and solvent use. For example, analysis time was decreased by 85% (42 h vs 6.3 h) for a nine-reaction experiment where each reaction was sampled at seven time points.[15] In addition, solvent use was decreased by 93%, due to the combined effects of lower flow rate and shorter analysis time, reducing both cost and environmental impact.

Development of a "One-Pot Process" To Prepare Semicarbazide 16. Application of in Situ ReactIR, FBRM, and PVM. A one-pot preparation and purification of semicarbazide **16** (Scheme 3) was developed to replace the three-step sequence outlined in Scheme 1. An earlier attempt[9] to develop a one-pot process starting with 4-methylbenzylhydrazine (**15**)[16] was unsuccessful due to an inability to separate **16** from its regioisomer **17**. Direct recrystallization from either IPA or EtOH gave no significant enrichment, and the mesylate salt of **16** was found to be unstable in alcoholic solvents at elevated temperatures. However, we have found that simple addition of aqueous HCl preferentially dissolves **17**, allowing **16** to be isolated directly by filtration (vide infra).

The initial process consisted of: (1) adding aqueous KOCN to a solution of **15**, (2) treatment of the resulting mixture of semicarbazides with a substoichiometric amount of aqueous HCl to preferentially dissolve **17** as its HCl salt, and (3) isolation of the desired product **16** by filtration. This process afforded **16** in 65% yield with 1.0−1.5% of **17**, and 0.5−3% each of **18**, **19**, and **20**. Hydrazone **18** and semicarbazone **19** were controlled by the rigorous exclusion of oxygen to prevent the facile oxidation of **15** to **2**. Attempts to improve the isomeric

Scheme 3. **One-pot preparation and purification of semicarbazide 16**[a]

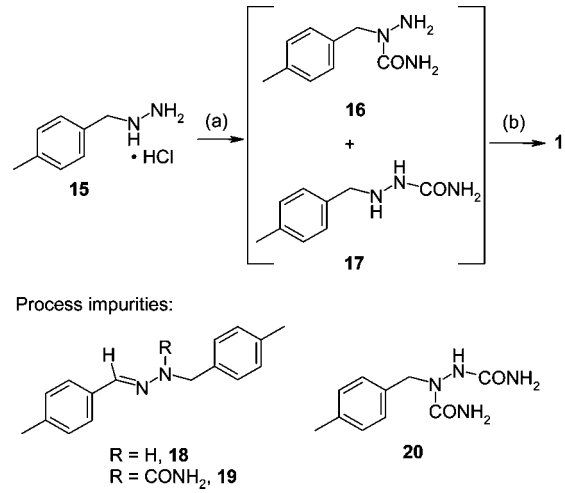

[a] Reagents and conditions for the optimized process: (a) KOCN (0.98 equiv), *n*-BuOH/H_2O (1:10 v/v), 20 °C, 8 h, 92% (not isolated, **16**/**17**, 80:20); (b) HCl (0.3 equiv), 20 °C, 3 h then filtered, 59% (**16**/**17**, 99.9:0.1).

ratio (which remained constant throughout the reaction) by varying the temperature[17] or the reaction solvent were not successful. This process was selected for further development due to its operational simplicity over the three-step process shown in Scheme 1.

There were three major development objectives for this step. First, the product partially floated, filling the reaction flask with solid. This is unacceptable in a manufacturing setting. Second, residual cyanate levels needed to be controlled since the presence of KOCN during the HCl addition resulted in the formation of **20**, an insoluble byproduct. Finally, a robust purification process was required to control the level of **17** consistently below 0.5%. The key role that process analytical technology (PAT) played in successfully addressing each of these issues is discussed below.

Microscopic analysis of the "floating" solid indicated that it consisted of microcrystalline agglomerates. Slowing the addition rate of aqueous KOCN and seeding the reaction mixture helped, but did not eliminate the problem. On the basis of observing that addition of approximately 10% IPA appeared to break up some of the particles, 18 water-miscible Class 2/3 solvents[18] were screened as reaction cosolvents in an attempt to improve crystallization performance. The best cosolvents were then compared using an automated Mettler Toledo MultiMax parallel reactor, where the distribution of particle chord lengths could be monitored using a Lasentec FBRM probe.[19] The dramatic influence of the cosolvent is illustrated in Figure 4, which shows significantly fewer, but larger, crystals when the cosolvent is

(15) See the Supporting Information for an illustration of the use of a data export method that enabled the preparation of nine multicomponent reaction profiles in less than 30 min from the raw data in 63 chromatograms.

(16) For preparation of the benzyl hydrazine from the corresponding chloride, see: Finneman, J. I.; Fishbein, J. C. *J. Am. Chem. Soc.* **1995**, *117*, 4228–4239.

(17) The ratios of **16**:**17** were: 82:18, 80:20, 76:24 at 5, 20, and 50 °C, respectively.

(18) *ICH Harmonised Tripartite Guideline. Impurities: Guideline For Residual Solvents QC3 (R3)*, revised November 2005. See: http://www.ich.org/cache/compo/363-272-1.html#Q3C.

(19) For useful discussions on the use of process analytical technology on crystallization processes, see: (a) Yu, L. X.; Lionberger, R. A.; Raw, A. S.; D'Costa, R.; Wu, H.; Hussain, A. S. *Adv. Drug Delivery Rev.* **2004**, *56*, 349–369. (b) Birch, M.; Fussell, S. J.; Higginson, P. D.; McDowall, N.; Marziano, I. *Org. Process Res. Dev.* **2005**, *9*, 360–364. (c) Barrett, P.; Smith, B.; Worlitschek, J.; Bracken, V.; O'Sullivan, B.; O'Grady, D. *Org. Process Res. Dev.* **2005**, *9*, 348–355.

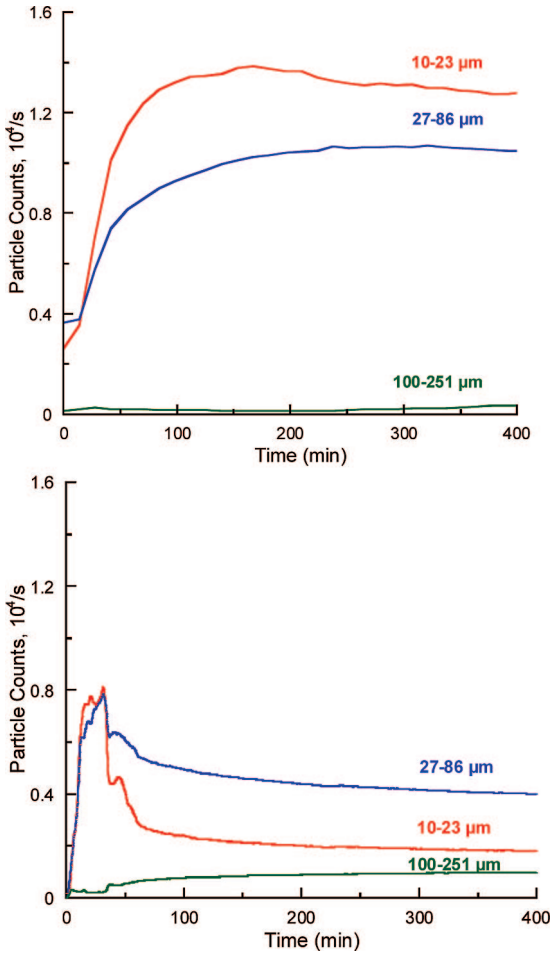

Figure 4. **Comparison of the FBRM profiles for the preparation of the semicarbazide mixture in H_2O (top) and 9% *n*-BuOH in H_2O (bottom). Both reactions were seeded.**

present. 1-Butanol (6−9% v/v)[20] was found to give large, dense crystals that rapidly settled out of solution and were easily filtered. In fact, the two isomers crystallized independently with different habits, the desired isomer **16** as rectangular plates and the undesired isomer **17** as bundles of rods. By contrast, small crystals remained throughout the course of the reaction when only water was used. The beneficial effect of a cosolvent does not appear to result from increased solubility, as both compounds are sparingly soluble in the reaction medium. (The solubility of **16** in H_2O and 1:10 *n*-BuOH/H_2O at 22 °C is 2.9 mg/mL and 3.9 mg/mL, respectively. The solubility of **17** in H_2O and 1:10 *n*-BuOH/H_2O at 22 °C is 1.1 mg/mL and 1.3 mg/mL, respectively.) Instead, it is possible that the cosolvent serves as a wetting agent that prevents the small crystals from agglomerating, thereby permitting larger-crystal growth to occur.

The second development objective, the control of residual KOCN to minimize the formation of **20** upon HCl addition, was also successfully addressed via PAT. In this case, online IR was used to measure in situ cyanate concentrations, which were then used in the development of a kinetic model for determining reaction completion. This approach provided a wealth of process knowledge with only a few experiments.

(20) Lower amounts of cosolvent resulted in agglomerates of smaller-sized crystals, while higher amounts of cosolvent (e.g., 15% v/v) resulted in a sticky solid and a biphasic filtrate.

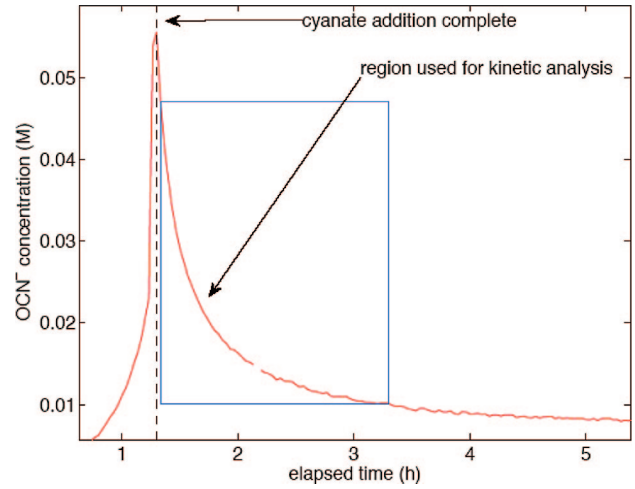

Figure 5. **Cyanate concentration as determined by IR versus elapsed time for kinetics experiment. The blue outline represents the subset of data used for kinetic modeling. The gap in the data line is due to a spectral measurement missed by the instrument.**

For developing the kinetic model, the reaction was carried out with a 2 mol % excess of cyanate, as described in the Experimental Section. IR data was collected throughout the course of the reaction. Following preprocessing, the spectral signal for cyanate was converted to concentration using the calibration model (Figure 5). The following three assumptions were made during our analysis. First, the reaction between cyanate and **15** is not measurably affected by equilibrium consideration, given the very low solubilities of **16** and **17** in the solvent system utilized.[21] Second, the reaction follows second-order kinetics overall between cyanate and **15**, and first-order in each reactant.[22] And third, hydrolysis of cyanate has only a small effect that does not significantly impact the overall findings.[23] Given these simplifying yet reasonable assumptions, we note that the concentration profile following cyanate addition can be used to extract kinetics information.

In order to extract the rate constant from the data, we take advantage of the self-similar nature of second-order kinetic profiles; any point in the profile can be chosen as an arbitrary initial condition, and the remaining points are calculated on the basis of that choice. (See Supporting Information for further discussion.) The measurements used for kinetic analysis include the first point following the peak cyanate concentration as the initial condition and all subsequent measurements having concentration values greater than or equal to the arbitrary cutoff value of roughly 0.01 M. We are assuming a concentration profile that obeys the following relationship.[24]

(21) Baker and Gilbert report that equilibrium is reached when 97% of hydrazine cyanate has reacted to semicarbazide in H_2O at 25 °C. However, in the present system, precipitation of the products would be expected to drive the reaction to completion: Baker, E. M.; Gilbert, E. C. *J. Am. Chem. Soc.* **1942**, *64*, 2777–2780.

(22) Williams, A.; Jencks, W. P. *J. Chem. Soc., Perkin Trans. 2* **1974**, 1753–1759.

(23) Kinetics for the aqueous hydrolysis of cyanate have been well characterized. For a recent reference with a summary of the literature, see: DeMartini, N.; Murzin, D. Y.; Forssen, M.; Hupa, M. *Ind. Eng. Chem. Res.* **2004**, *43*, 4815–4821.

(24) Levenspiel, O. *The Chemical Reactor Omnibook*, Oregon State University Bookstores: Corvalis, OR, 1996; p 2.3.S. and subsequent manipulation in the Supporting Information.

$$\frac{[A]}{[A]_0} = \frac{M-1}{M\rho - 1},\ \rho = \exp(k[A]_0(M-1)t)$$

Here, species A refers to cyanate, and the initial concentration is obtained directly from the processed IR signal. The value of M, which is the molar ratio of **15** to cyanate at the initial point, is calculated from the initial molar ratio and conversion of cyanate. With a cost function defined as the sum of squares of the residuals between the kinetic model and the measured data, a function minimization routine[25] generated a rate constant of 90 M^{-1} h^{-1} as optimal (Figure 6). Extending the optimization out further had minimal impact on the value of the rate constant; including all data points to the end of the measurement period resulted in an optimal value of k of 88 M^{-1} h^{-1}.

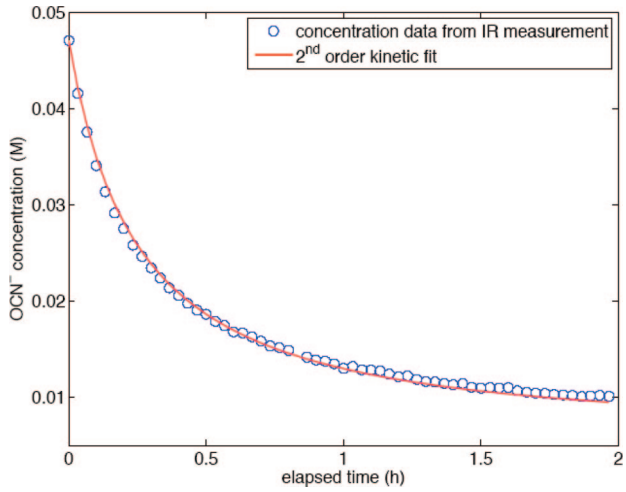

Figure 6. **Fit of experimental data to the kinetic model. The rate constant was determined by nonlinear least-squares.**

The reaction scheme depicted for this step, beginning with the semibatch period where the cyanate solution is added at a constant rate over a predetermined period of time followed by a constant-volume batch reaction is readily modeled (see Supporting Information for development of the model). In practice, cyanate will be the limiting reagent, but reversing the roles for the present experiment affords more data to use for fitting to a kinetic model without the concern of running up against limit of quantitation considerations. Once the rate equations for cyanate and **15** are made dimensionless and the initial conditions are simplified through variable substitution, only the following three adjustable parameters remain: M, as defined above; β, the ratio of the initial reaction volume to that of the cyanate solution to be added; and α, the product of (1) the rate constant, (2) the time for the cyanate addition (units consistent with that of the rate constant), and (3) the concentration of cyanate in the dosing solution.

In practice, KOCN will be the limiting reagent (with 2 mol % excess **15**), and β will be very close to 8. The time for cyanate conversion to reach completion as predicted by the model is shown in Table 1 for three different cyanate addition times (t_{fill}). Under these conditions, cyanate is essentially consumed (99.9% conversion) within 5−6 h. Little penalty is observed in extending the addition time from 0.25 to 1 h in order to achieve the improved crystal growth mentioned earlier.

(25) MATLAB function `fminbnd`: This algorithm uses golden section search and parabolic interpolation.

Scheme 4. **Equilibria for the separation of 16 and 17**

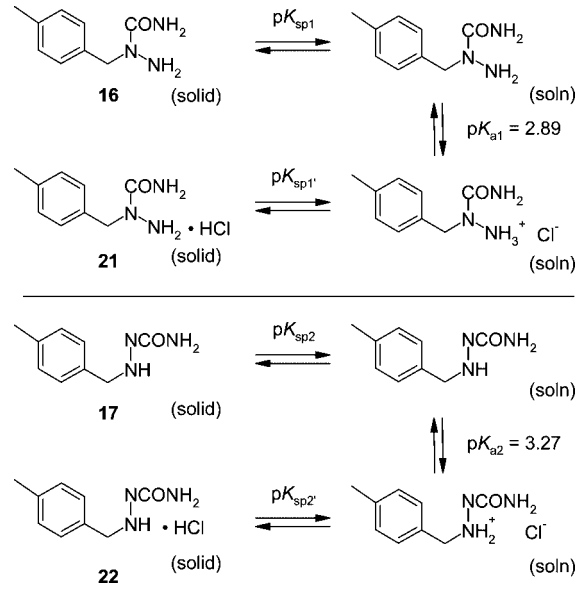

Table 1. **Predicted reaction times for cyanate conversion to reach >95% with KOCN addition times of 0.25 h, 0.5 h, and 1 h (20 °C, 2 mol % excess of 15)**

OCN^- conversion (%)	time (h) (t_{fill} = 0.25 h)	time (h) (t_{fill} = 0.5 h)	time (h) (t_{fill} = 1 h)
95.0	0.70	0.90	1.30
99.0	1.95	2.16	2.59
99.5	2.79	3.00	3.43
99.9	5.14	5.35	5.78

The ability to model the time for reaction completion using only fill time, temperature, and stoichiometry allows the level of cyanate to be controlled to less than 0.5% prior to the addition of HCl, thereby maintaining the levels of biscarboxamide **20** below this value. Importantly, this can be now accomplished in manufacturing without the need for an in-process control assay for cyanate or online monitoring.

The final objective for this step was to develop a robust purification. Once again, PAT played an important role, with data from both FBRM and particle vision and measurement (PVM) probes providing key insights for improving the process.

As mentioned above, **16** was purified by treatment of the semicarbazide mixture with aqueous HCl. The equilibria involved in this process are shown in Scheme 4. The preferential dissolution of isomer **17** is the result of two factors, its higher basicity (the pK_a for ammonium salts **22** and **21** are 3.27 and 2.89, respectively, in MeOH/H_2O at 25 °C) and a 50% greater solubility of **22** compared to **21**. However, the initial process was not robust. Levels of **17** varied from 0.1−1.2% and were strongly dependent upon the washing protocol employed, even when the HCl stoichiometry was increased.

In situ monitoring using a Lasentec FBRM probe during the HCl addition enabled us to quickly determine the origin of the variability. As 5 N HCl was added to the slurry, a decrease in the number of larger particles was observed with the dissolution of **17**. Unexpectedly, a sharp increase occurred in the number of small particles (Figure 7, red line), along with the simultaneous appearance of numerous, hair-like crystals

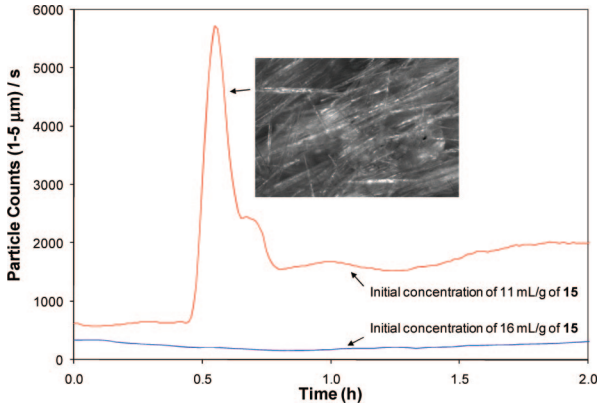

Figure 7. **Comparison of FBRM profiles for reactions conducted at two different concentrations. Photo insert shows the hair-like crystals of 22, which were only observed at the higher concentration.**

in the PVM (see photo insert in Figure 7). The small crystals were not visible to the naked eye. They decreased in number as the acid was added but remained throughout the equilibration step. Apparently, as **17** was protonated, the solution concentration of **22** exceeded its solubility, and it began precipitating. As the addition proceeded, the reaction mixture became more dilute allowing some of the precipitated **22** to redissolve. This explains the cause for the variability observed in the product purity and its dependence on the washing protocol. The isomer was being removed not only by expressing the filtrate from the filter cake but also by redissolution of precipitated **22** that was contained within the cake. Once understood, the variability was readily eliminated by simply increasing the amount of solvent from 11 mL/g of **15** to 16 mL/g; thereby ensuring that **22** remained in solution (Figure 7, blue line). This modification significantly improved the process robustness, enabling the level of **17** to be controlled consistently below 0.2% at both laboratory and pilot-plant scale, albeit with a slight decrease in yield to 59% due to increased product loss to filtrate.

Development of the Monoalkylation Process to Prepare Carboxylic Acid 5. Carboxylic acid **5** was prepared by monoalkylation of the dianion of **4** with ethyl 2-bromoisobutyrate (EBIB), as shown in Scheme 1. Our two primary objectives were (1) development of a control strategy for the four API impurities (**11**−**14**) that originated from this step and (2) development of an improved isolation/purification process. Fortunately, the levels of **12**−**14** could all be controlled to less than 0.1% by setting appropriate specifications on the alkylating agent EBIB. The other API impurity, phenol **11**, which originated from the carry-though and forward processing of unreacted starting material **4**, was reduced to less than 0.1% via the modified workup described below.

The alkylation reaction was conducted as described by Schmid and co-workers.[9] This process gave a reaction profile consisting of the desired acid **5** and 1−2% each of **10** and **4**, as well as excess alkylating agent and ethyl methacrylate from the dehydrobromination of EBIB. In addition, the crystallization of **5** from acidic aqueous EtOH was no longer acceptable due to poor impurity rejection and a tendency for the product to oil.

The isolation was modified by quenching the reaction into a mixture of toluene and aqueous HCl. The product could be extracted directly from the aqueous EtOH upon adjustment of the pH to less than 2, or it could be separated from the neutral organic byproducts by adjustment of the pH to 7−9, followed by extraction into toluene upon acidification. The latter process was preferred because it provided both an inherently safer and a more robust process. Removal of the potentially polymerizable ethyl methacrylate avoided the safety issues associated with its concentration during the crystallization process. In addition, ethyl methacrylate and unreacted EBIB solubilized the product and led to variability in the crystallization yield. The new process using toluene afforded two additional advantages. It allowed both impurities **10** and **4** to be quantitatively removed by an aqueous extraction containing 5−7 mol % $NaHCO_3$, thereby eliminating API impurity **11**. It also enabled the development of a robust crystallization of **5** from toluene/heptane with improved impurity rejection on a multikilogram scale (4 × 18 kg lots, 86 ± 1% yield, 0.2 ± 0.1% total related substances (TRS)).

Development of the Process to Prepare Triazolone 8. Application of DoE, UPLC, and FBRM. Preparation, purification, and isolation of triazolone **8** was one of the primary quality control points for the entire synthetic route. As shown in Scheme 1, it was prepared by first coupling acid chloride **6** with semicarbazide **16** to give acylsemicarbazide **7**. This product was carried forward without isolation, since it was formed in nearly quantitative yield, and all attempts to filter the crystalline product were unsuccessful.[26] Addition of CSA at reflux affected the cyclization to **8**, as described by Schmid and co-workers,[9] albeit with several byproducts that could not be rejected by crystallization (vide infra).

The three primary development objectives for this sequence were as follows: first, replacement of DMF as a catalyst in the acid chloride formation, as it gives rise to API impurity **9**; second, improvement of the impurity control strategy, eliminating the need for treatment with Amberlyst 15 resin prior to crystallization; and finally, development of a controlled, robust crystallization process.

DMF was replaced with pyridine in the acid chloride formation. Carson and Reist[27] have shown that pyridine is a highly effective catalyst for the formation of acid chlorides, while suppressing anhydride formation. We compared the activity of DMF and pyridine as catalysts in the conversion of **5** to **6** via oxalyl chloride in toluene. Pyridine was found to give essentially identical results over the range tested (0.1−5.0 mol %), with two quality benefits: elimination of the problematic chloroiminium species formed with DMF, and lighter-colored reaction mixtures (light-yellow vs yellow-brown). Symmetrical anhydride was not detected with either catalyst. A catalyst loading of 0.1 mol % pyridine was selected and the process was optimized using a fractional factorial experimental design varying the following three parameters: oxalyl chloride stoichiometry, reaction concentration, and temperature (see Supporting Information). Excess oxalyl chloride was removed by

(26) Treatment of acylsemicarbazide **7** with aqueous NaOH (20 h at 40 °C followed by 24 h at 100 °C), using conditions similar to those described in ref 5c, affords LY518674 (**1**) in a single step (77% yield). However, isolation and purification of **8**, followed by saponification to give **1**, provides a better impurity-control strategy than the one-step process.

(27) Carson, J.; Reist, E. J. *J. Org. Chem.* **1958**, *23*, 1492–1496.

Scheme 5. **Impurities derived from 7**

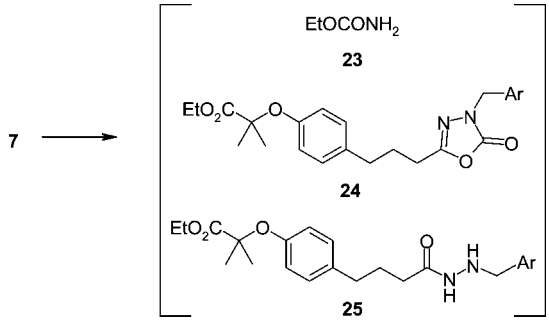

distillation, using online vapor-phase MS analysis of the distillate to monitor the removal during pilot-plant production.

Acylsemicarbazide **7** was prepared in nearly quantitative yield by addition of the resulting acid chloride solution to a slurry of semicarbazide **16** in toluene containing pyridine, which served as both a base and an acylation catalyst. Acid was then added directly to the crude reaction mixture to effect the cyclization.

10-Camphorsulphonic acid was found by Schmid to be preferred for promoting the cyclization of **7** to triazolone **8**.[9] An excess of CSA (1.7 equiv) was used to keep the reaction rate from slowing dramatically, as the imine nitrogen in the product ($pK_a \approx 2.8$) was protonated under the strongly acidic conditions. Typically the reaction was complete after 3 h at 100 °C or 17 h at 70 °C. Similar product profiles were obtained at both temperatures: triazolone **8** (60−70%), hydrazide **25** (10−15%), API **1** (5−10%), carboxylic acid **5** (5−10%), and oxadiazolone **24** (2%), along with several smaller impurities (Scheme 5). The 5-min UPLC assay described earlier dramatically aided the development of this reaction sequence, as the origin and fate of over 30 components needed to be understood.

Hydrazide **25** was the most problematic impurity. Previously, it had been removed by adsorption on Amberlyst 15 resin, as it was not rejected by crystallization and was poorly removed by acidic extraction. Furthermore, it was not possible to reduce the levels of this impurity, as cleavage of the carboxamide group in **7** is surprisingly facile, occurring under both acidic and basic conditions and at temperatures above 100 °C. We suspect this lability arises from anchimeric assistance by the oxygen of the internal amide group. Unfortunately, attempts to verify this hypothesis via NMR detection of the putative *O*-acyl intermediate were unsuccessful.

The critical discovery for impurity control in this process was somewhat counterintuitive, namely, addition of a strong acid (HCl or H_2SO_4) with EtOH to the crude reaction mixture and heating at reflux.[28] This converted numerous impurities that could not be rejected by crystallization into a smaller number of components that were readily rejected by either extraction or crystallization. API **1** was esterified to give **8**. All amide-containing species and unreacted **5** were converted into diethyl ester **28** which was readily rejected by crystallization (Scheme 6). The 4-methylbenzyl hydrazine **26**, liberated from **7**, **16**, and **25** reacted with CSA to give hydrazone **27**, which was readily removed by extraction. The only components stable to the ethanolysis conditions were the desired product **8** and oxadiazolone **24**, which was readily rejected by crystallization. This control strategy is so efficient that any amount of compounds **1**, **5**, **7**, **16**, **24**, and/or **25** can be present *without any impact to the quality* of triazolone **8** obtained from the crystallization.

Scheme 6. **Control of impurities**

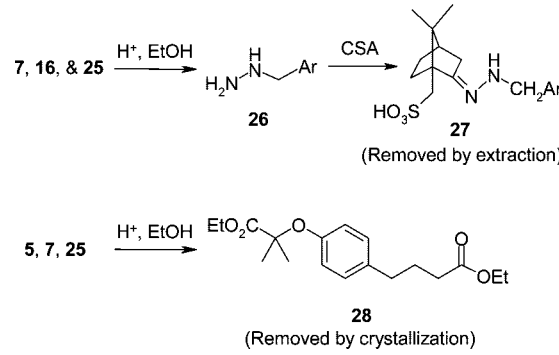

The use of EtOH in the presence of H_2SO_4 gave rise to three, potentially genotoxic impurities that were readily controlled. The ethyl sulfonate ester derived from CSA was rejected in the crystallization. Urethane (**23**), a known animal carcinogen formed from ethanolysis of **7** and **16**, was removed in both the aqueous washes and the crystallization step. Finally, monoethyl sulfate ($EtOSO_3H$), formed by esterification of H_2SO_4,[29] was removed in the aqueous $NaHCO_3$ wash. Although the latter could be eliminated by the use of anhydrous HCl, the use of a liquid acid was deemed preferable for safety and simplicity in handling at large scale.

Use of toluene as the reaction solvent for the three-step sequence permits direct crystallization of triazolone **8** after aqueous workup, upon concentration and addition of *n*-heptane, without the need for a solvent exchange. Due to the strong temperature dependence of the solubility of **8** in 1:2 toluene/heptane,[30] we felt a more robust crystallization could be achieved by an initial antisolvent addition followed by cooling. After concentration of the toluene solution, *n*-heptane was added at 45 °C giving a 65:45 ratio (v/v) of toluene/heptane. The solution was seeded at 37 °C (∼30% supersaturation), and the remaining heptane was added over 2.5 h, resulting in a 33:67 ratio (v/v) of toluene/heptane. Data from the Lasentec FBRM probe (Figure 8), indicate that most of the crystal growth occurred during the antisolvent addition. These data also show that no change in the distribution of particle chord lengths occurred as the slurry was cooled from 37 to 10 °C over 3 h. The product precipitated as clear, rectangular plates that filtered rapidly. Data from the FBRM probe also showed that no

(28) It is well-known that ethyl hydrogen sulfate ($EtOSO_3H$) is formed upon reaction of H_2SO_4 with EtOH. For kinetic studies, see: (a) Theodore, S.; Sai, P. S. T. *Can. J. Chem. Eng.* **2001**, *79*, 54–64. (b) Chen, L.; Johnson, B. D.; Grinberg, N.; Bicker, G. R.; Ellison, D. K. *J. Liq. Chromatogr. Relat. Technol.* **1998**, *21*, 1259–1272. (c) Clark, D. J.; Williams, G. *J. Chem. Soc.* **1957**, 4218–4221. (d) Deno, N.; Newman, M. *J. Am. Chem. Soc.* **1950**, *72*, 3852–3856.

(29) A stock solution of 2.5 M H_2SO_4 in EtOH exists as an 80:20 mixture of $EtOSO_3H$ and H_2SO_4, based upon integration of the quartets at 4.2 ppm and 3.8 ppm, respectively. The equilibrium ratio is a function of the amount of water present. Diethyl sulfate (q, 4.3 ppm) is not formed under these conditions, and when spiked into the solution it is converted to the monoethyl sulfate. Lit. for ^{1}H NMR shift for $HO_3SO^{13}CH_2CH_3$ 4.25 ppm (dq): Sen, A.; Benvenuto, M.; Lin, M.; Hutson, A.; Basickes, N. *J. Am. Chem. Soc.* **1994**, *116*, 998–1003.

(30) Plots of the solubility vs temperature and solubility vs percent of *n*-heptane are included in the Supporting Information.

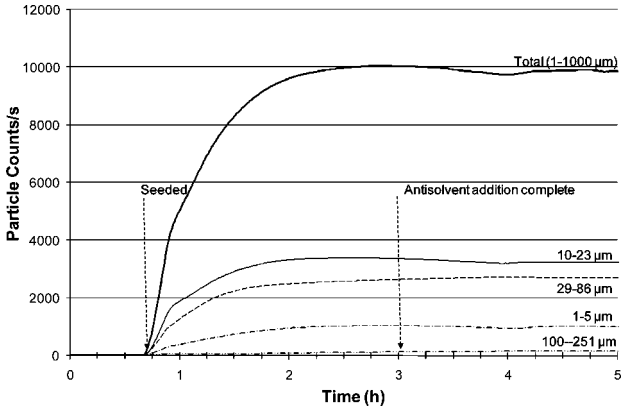

Figure 8. **In situ FBRM data collected during crystallization of 8.**

attrition of the crystals occurred upon prolonged stirring (8 h), but only the first two hours of data are included in Figure 8.

The robustness of the control strategy was demonstrated in three, 7 kg pilot-plant lots that afforded triazolone **8** in 64 ± 1% yield and with total related substance levels of 0.33 ± 0.02% for the three-step sequence.

Development of the API Crystallization. Development of the final step was straightforward, saponification of **8** with aqueous NaOH at room temperature followed by crystallization of LY518674 (**1**) from EtOAc (Scheme 1). It was found that a biphasic hydrolysis, as described in the original protocol, was not required, so toluene was removed. However, addition of the EtOAc *prior to neutralization* was found to be highly advantageous, keeping the product in solution throughout the acidification process. LY518674 (**1**) contains three ionizable groups with pK_a values of 9.0 (triazolone ring (N-4)), 3.8 (carboxylic acid), and 2.8 (triazolone ring (N-1)).[31] The monoanion is only sparingly soluble and tended to form a gum at around pH 7 if the organic solvent was not present.

Ethyl acetate, an ICH Class 3 solvent,[32] is uniquely suited for use in both the extraction and the crystallization. The EtOH released by the hydrolysis of both EtOAc and **8** dramatically increased the solubility of the product in the organic layer, thereby minimizing processing volumes.[33] Yet upon removal of water and EtOH by distillation, LY518674 was isolated in 96% yield via a seeded, temperature-controlled crystallization process.

Technology played a key role in our ability to rapidly optimize the API crystallization process. The Crystal16 automated solubility station by Avantium Technologies was used to determine the impact of water, EtOH, and HOAc on product solubility. It was found that stopping the distillation with 13 volumes of solvent and less than 0.4% H_2O ensured that spontaneous nucleation would not occur above 70 °C and that

(31) The pK_a values were measured by potentiometric titrations at three concentrations of dioxane water and extrapolating to pure water using a Yasuda−Shedlovsky plot. Baertschi, S.; et al. Unpublished results, Eli Lilly and Company.

(32) Residual levels up to 0.5% are acceptable for Class 3 solvents without justification (ref 18).

(33) At 23 °C, the solubility of **1** is 3.7 mg/mL in anhydrous EtOAc vs 38.1 mg/mL in water-saturated EtOAc and 100 mg/mL in water-saturated EtOAc containing 2 wt % EtOH (see ref 9). Acetic acid is also formed during the hydrolysis of EtOAc but does not significantly impact the solubility of **1** in EtOAc.

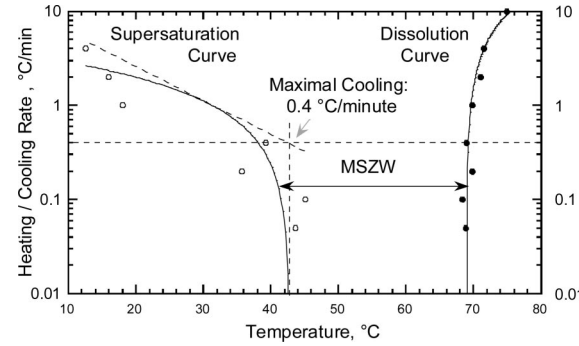

Figure 9. **Influence of the crystallization cooling rate on the MSZW at a concentration of 1 g LY518674 per 13 mL of EtOAc.**

less than 4% product would be lost to the filtrate. Levels of HOAc and EtOH were typically 0.69% (w/w) and 0.03% (w/w), respectively and were very consistent.

Knowledge of the metastable zone width (MSZW), the difference between the dissolution and spontaneous nucleation points as a function of a solubility-influencing parameter such as temperature and at given substrate load, is critical to design a robust crystallization process.[34] This system possesses a broad MSZW and a steep solubility/temperature dependence with a high supersaturation level (471%), even in the midpoint of MSZW. Seeding, therefore, became indispensable for such a system to start a heterogeneous nucleation at the desired supersaturation ratio to prevent very heavy, yet uncontrollable, nucleation from happening. The MSZW is also a function of the cooling rate as shown in Figure 9, increasing significantly at rates above 0.4 °C/min. The optimum crystallization conditions consisted of seeding (1% w/w load) at 60 °C (30% supersaturation) followed by cooling at a rate of 0.2 °C/min to 5 °C. Control of the crystallization process was also essential for obtaining reproducibly low levels (<0.2%) of residual EtOAc in the API, which varied from 0.5−1.5% at cooling rates above 0.5 °C/min and if the crystallization process was not seeded.

Implementation of the process at 0.1−4.5 kg scale afforded LY518674 (**1**) in 95.4 ± 0.6% yield from **8**. The crystallization process proved to be quite robust, giving comparable product from three lots, both in terms of its chemical purity (0.18 ± 0.02% TRS) and its physical properties (d_{90} (128−160 μm), d_{50} (38−58 μm), d_{10} (12−19 μm)). Importantly, the high product quality obtained directly from the initial crystallization obviates the need for a recrystallization, thereby eliminating any additional risk of worker exposure to the highly potent API.

Conclusions

Several new technologies were used during the development of a manufacturable route for PPARα agonist LY518674 (**1**). Their use allowed for a higher level of process knowledge to be obtained during development while simultaneously increasing productivity. As a result, a control strategy was developed in which all six API impurities (**9**−**14**) were controlled to below

(34) Mersmann, A., Ed. *Crystallization Technology Handbook*, 2nd ed.; Marcel Dekker: New York, 2001.

the ICH reporting threshold of 0.05%.[35] Furthermore, the acquired process knowledge enabled quality to be designed into each step such that the total impurity load for each synthetic intermediate was less than 0.5%.

The combination of sub-2 μm column technology and the higher pressures accessible with the Waters ACQUITY UPLC greatly increased analytical efficiency by allowing over 30 components to be tracked with a single, 5-min, MS-friendly assay throughout the four-step process. Further productivity gains were achieved with the use of chromatography-modeling software to aid method development and data export methods to expedite the conversion of chromatography data into multicomponent reaction profiles.[15]

Process analytical technology (PAT), such as online IR, PVM, FBRM, and MS played a key role in acquiring the process knowledge needed for development of the control strategy and in allowing comparison of the process performance at laboratory and pilot-plant scale. Importantly, the knowledge gained will permit subsequent scaleup to occur *without the requirement of PAT for process control*, except in instances where doing so will limit worker exposure (e.g., monitoring of drying operations by online MS).

Experimental Section

General. All reactions were run under a nitrogen atmosphere, unless otherwise specified. Reagents were used as received unless otherwise noted. Proton NMR spectra were obtained at 400 MHz and carbon NMR spectra were obtained at 100.6 MHz. NMR chemical shifts are reported in δ units referenced to residual proton signals in the deuterated solvent. All yields are corrected for chemical purity of both the limiting reagent and the product (i.e., yield = (weight of product × purity/MW of product)/(weight of limiting reagent × purity/MW of limiting reagent) × 100). If the purity of a product is not specified, it is greater than 99%. Analytical methods used for reaction monitoring and purity determination are described in the Supporting Information.

Development of the Kinetic Model for Formation of 16. The reaction was conducted in a Mettler AutoChem RC1e reaction calorimeter with an 800-mL glass vessel equipped with a ReactIR 4000 FTIR with a SiComp attenuated total reflectance probe sensor. Calibration was achieved using freshly prepared standard solutions of KOCN in an *n*-BuOH:H_2O solvent system matching that used in the reaction at 20 °C. The cyanate profile was generated by integrating over the spectral range of 2088−2254 cm^{-1} after spectral preprocessing to remove the underlying water absorbance. The resulting calibration plot exhibits a significant departure from linearity but is amply fit by a quadratic function. See the Supporting Information for details on the calibration and determination of the limits of detection and quantitation. IR data were collected throughout the course of the reaction. Following preprocessing, the spectral signal for cyanate was converted to concentration using the calibration model.

Water (455 mL) and 1-butanol (33.5 mL) were mixed. Argon was sparged through the solution for approximately 20 min to remove oxygen prior to adding **15** (33.10 g, 191.7 mmol, 1.0 equiv), after which it was deoxygenated for an additional 5 min.

A solution of KOCN (16.20 g, 98% assay, 195.7 mmol, 1.02 equiv) in deoxygenated H_2O (61 mL) was added over 60 min. Ten minutes into the addition, the reaction was seeded with **16** (0.300 g, 1.67 mmol). When the addition was complete, the lines were rinsed with deoxygenated H_2O (19.4 mL), and the slurry was stirred overnight at 20 °C.

Note: A 2 mol % excess of KOCN was used to avoid concerns of approaching the limit of quantitation throughout the reaction, whereas it is the limiting reagent under the standard conditions. In addition, the *n*-BuOH:H_2O ratio was reduced from 9:1 to 6.3:1.0 (v/v) to ensure miscibility of the two solvents throughout the reaction.[36]

Development of the API Crystallization Process. The research was conducted using an Avantium Technologies Crystal16 automated solubility station. This is a medium-throughput screening tool having a 4 × 4 array of 16 1.5 mL microreactor vials, permitting the rapid acquisition of information with minimal material requirements. Each microreactor is equipped with a light-emitting diode (LED) and photosensor for measuring turbidity in transmission (through the sample) to determine dissolution point. The Crystal16 automated solubility station was used to acquire solubility information and to define the dependence of the MSZW on the cooling rate.

A Mettler Toledo MultiMaxIR automated parallel reactor system equipped with a focused-beam reflectance measurement (FBRM) probe was used for larger-scale crystallization development for better simulation of process equipment and parameters.

1-[(4-Methylphenyl)methyl]hydrazinecarboxamide (16). *Caution!* Aqueous solutions of KOCN are subject to autocatalytic hydrolysis and should not be stored.[37] All solutions were prepared immediately prior to use and were maintained at 20 °C in a jacketed vessel at all times. Note: It is important to deoxygenate all solutions prior to use and to conduct the reaction under an inert atmosphere to prevent oxidative degradation of **15**.[38]

(4-Methylphenyl)hydrazine hydrochloride (11.5 kg, 66.6 mol, 1.02 equiv)[16] was added to a deoxygenated solution

(35) *ICH Harmonised Tripartite Guideline. Impurities in New Drug Substances Q3A (R2)*, revised October 2006. Available on-line at: http://www.ich.org/cache/compo/363-272-1.html#Q3A(R).

(36) (a) For a discussion of the liquid-liquid-solid equilibria for the ternary system of *n*-BuOH/water/KCl, see: (b) Gomis, V.; Ruiz, F.; Asensi, J. C.; Saquete, M. D. *J. Chem. Eng. Data* **1996**, *41*, 188–191.

(37) (a) For a detailed investigation of an explosion of 30% aqueous KOCN that occurred in a vented drum, see: Pinsky, M. L.; Vickery, T. P.; Freeman, K. P. *J. Loss Prev. Process Ind.* **1990**, *3*, 345–348. (b) A major factor in the drum explosion was the heating of the aqueous mixture to 50 °C in order to dissolve all of the solids, prior to storage. However, calorimetry experiments demonstrated that a 30% aqueous solution of KOCN is unstable even at room temperature, reaching its maximum decomposition rate after 30 h at 25 °C due to autocatalysis by HCO_3^-. See also: Urben, P. G., Ed. *Bretherick's Handbook of Reactive Chemical Hazards*, 6th ed.; Butterworth-Heinemann: Oxford, Boston, 1999; Vol. 1, pp 201−202.

(38) Oxygen must be excluded from all process streams to minimize formation of the insoluble hydrazone **18**, resulting from reaction of 4-methylbenzaldehyde (from the oxidation of **15**) with **16**, and semicarbazone **19**, resulting from its subsequent reaction with KOCN. Solutions were deoxygenated by purging them with N_2 (1.18 ft^3 N_2 L^{-1} of solution) to an O_2 level of approximately 0.4 ppm. Initial O_2 levels ranged from about 9 ppm in the laboratory to 3.4 ppm in the pilot plant. Typically, 0.5 h was required for the deoxygenation of laboratory runs, and approximately 1 h was required for deoxygenation in the pilot plant.

containing *n*-BuOH (3.94 kg, 17.21 L) and H_2O (154 L) at 20 °C. The solution was transferred through a 0.45 μm in-line filter,[39] and the line was rinsed with deoxygenated H_2O (6.0 L). A deoxygenated aqueous solution of KOCN was prepared by adding KOCN (5.60 kg, 94.3% assay,[40] 65.1 mol, 1.0 equiv) to H_2O (21.0 L) with stirring at 20 °C and purging the resulting solution with N_2.

The aqueous KOCN was added to the hydrazine solution at 20 °C in two portions in order to saturate the reaction mixture with product prior to seeding. The first portion (0.12 equiv) was added over 10 min, and the reaction was stirred for 0.75 h. The reaction was then seeded with a slurry of **16** (0.1 kg, 0.56 mol, 0.008 equiv) in *n*-BuOH (0.10 L) and H_2O (0.40 L). The container was rinsed with H_2O (0.80 L). The remaining aqueous KOCN was added at a rate of 0.016 equiv/min until 60% of the total KOCN had been added. The rate was slowed to 0.0046 equiv/min during the remainder of the addition, giving a total addition time of 2 h.[41] The combination of solvent composition and addition rate permits the two isomeric products to crystallize independently. The line was rinsed with deoxygenated H_2O (6.0 L), and the reaction slurry was stirred for 12 h at 20 °C.[42] The reaction is quantitative giving a slurry containing an 80:20 mixture of the desired semicarbazide **16** and the isomeric **17**, respectively.

Hydrochloric acid (3.89 L of 5.04 M, 0.30 equiv) was added to the slurry (pH 8.83) at 20 °C to dissolve the undesired isomer. The transfer line was rinsed with H_2O (7.3 L), and the reaction mixture was stirred for 3 h at 20 °C (final pH 2.31). The slurry was filtered, and the wet cake was washed with 35 °C H_2O (3 × 27.5 L). The product was dried overnight at 60 °C/100 mmHg to give 7.045 kg of **16** (58.6% yield, 98.4% assay, 0.07% H_2O, 0.11% **17**, 0.10% **20**)[43] as a white solid, mp 152.5−155.2 °C. Anal. Calcd for $C_9H_{13}N_3O$: C, 60.32; H, 7.31; N, 23.45; O, 8.93. Found: C, 60.31; H, 7.20; N, 23.38. ^{1}H NMR (DMSO-d_6: δ 2.25 (s, 3H), 4.20 (s, 2H), 4.18 (s, 2H), 6.10 (br s, 2H), 7.10 (m, 4H). ^{13}C NMR (DMSO-d_6: δ 21.1, 52.3, 128.3 (2C), 129.4 (2C), 135.4, 136.5, 160.5. IR (KBr): 3424, 3333, 3045, 3023, 2978, 2361, 2333, 1907, 1653, 1576, 903, 846 cm^{-1}. HRMS (*m*/*z* M + 1): Calcd for $C_9H_{14}N_3O$: 202.0951. Found: 202.0946.

4-(2-Ethoxy-1,1-dimethyl-2-oxoethoxy)benzenebutanoic Acid (5). 4-Hydroxyphenylbutanoic acid (13.06 kg, 72.48 mol, 1 equiv)[10] and EtOAc (6.6 kg, 74.9 mol, 1.03 equiv)[44] were added to NaOEt (46.88 kg of 21% NaOEt in EtOH, 144.7 mol, 2 equiv) at 25 °C. The resulting slurry was heated at reflux (76.8 °C) for 1 h. Ethyl 2-bromoisobutyrate (31.8 kg, 163.0 mol, 2.25 equiv) was added. An additional charge of NaOEt (23.6 kg of 21% NaOEt in EtOH, 72.8 mol, 1 equiv) was added over 1 h.[45] When less than 1% starting material remained by HPLC, the reaction mixture was cooled to 25 °C and transferred into a mixture of aqueous 0.5 N HCl (3.72 kg 35% HCl, 35.7 mol, 0.5 equiv + 68 kg of H_2O) and toluene (65 L) at 22 °C. The pH was adjusted from 6.55 to 8.39 with the addition of 50% NaOH with stirring. After phase separation, the aqueous phase was washed with toluene (65 L). Toluene (130 L) was added, and the pH of the aqueous phase was adjusted from 8.77 to 1.99 by the addition of HCl (13.4 kg of 35% HCl, 128.6 mol, 1.77 equiv) with stirring at 23 °C. The organic phase was washed sequentially with H_2O (66 L) and 0.078 M $NaHCO_3$ (0.44 kg, 5.24 mol, 0.07 equiv in 67 L of H_2O).[46] The organic layer was concentrated to approximately 6 volumes by vacuum distillation. After cooling to 20 °C, heptane (40 L) was added, followed by seed crystals of **5** (0.19 kg, 0.64 mol, 0.09 equiv) and the resulting slurry was stirred for 0.5 h. Additional heptane (175−180 L) was added with stirring over at least 3 h. The resulting slurry was stirred at 20 °C for 2 h and at 2 °C for 2 h prior to filtration. The wet cake was washed with 6:1 (v/v) heptane/toluene (2 × 35 L). Acid **5** (18.64 kg, 99.0% assay, 99.76% purity, 86.3% yield) was obtained as an off-white powder after vacuum drying for approximately 12 h at 45 °C/100 mmHg, mp 70.6−71.5 °C. Anal. Calcd for $C_{16}H_{22}O_5$: C, 65.29; H, 7.53; O, 27.18. Found: C, 65.18; H, 7.37. ^{1}H NMR (DMSO-d_6: δ 1.14 (t, J = 7.3 Hz, 3H), 1.47 (s, 6H), 1.73 (quintet, J = 7.5 Hz, 2H), 2.17 (t, J = 7.5 Hz, 2H), 2.47−2.51 (m, 2H), 4.13 (q, J = 7.1 Hz, 2H), 6.69−6.70 (m, 2H), 7.04−7.07 (m, 2H), 12.01 (s, 1H, D_2O exch). ^{13}C NMR (DMSO-d_6: δ 14.3, 25.5 (2C), 26.8, 33.5, 34.0, 61.4, 79.0, 119.3 (2C), 129.5 (2C), 135.6, 153.6, 173.7, 174.7. IR (KBr): 3443, 3072, 3003, 2977, 2926, 1733, 1704, 1610, 1582, 642, 591 cm^{-1}. HRMS (*m*/*z*, M + 1): Calcd for $C_{16}H_{23}O_5$: 295.1540. Found: 295.1532.

2-[4-[3-[2,5-Dihydro-1-[(4-methylphenyl)methyl]-5-oxo-1H-1,2,4-triazol-3-yl]propyl]phenoxy]-2-methylpropanoic Acid, Ethyl Ester (8). *Caution!* PPARα agonist LY518674 (**1**) and its ester derivative **8** are highly potent compounds[5,8] and should be handled with extreme caution to prevent worker exposure.

Oxalyl chloride (2.25 kg, 17.7 mol, 1.20 equiv) was added to a solution of **5** (4.33 kg, 14.71 mol, 1.00 equiv), pyridine (1.2 mL, 0.015 mol, 0.0010 equiv), and toluene (25 L) at 22 °C over 10 min. The lines were rinsed with toluene (1 L) and the reaction was stirred for at least 1.5 h until less than 0.5% of the starting acid remained.[47] The reaction was concentrated to approximately 8−10 L by vacuum distillation (~60 °C/100−150 mmHg) to remove excess oxalyl chloride.

(39) In-line filtration removes any hydrazone impurity that formed due to oxidative degradation of the starting hydrazine.
(40) The KOCN also contains 0.6% K_2CO_3 (w/w). The assay for KOCN was determined by acid-base titrations using vendor-provided procedures. The assay is a two-part procedure. Part 1 involves titration of residual potassium carbonate (K_2CO_3) vs H_2SO_4. Part 2 involves heating a cyanate solution with H_2SO_4, followed by a back-titration of excess (unreacted) H_2SO_4 with sodium hydroxide. Final results are calculated by subtracting the amount of K_2CO_3 from the titration results in Part 2.
(41) The KOCN solution may be added at a constant rate over 1 h.
(42) The reaction time can be determined using the kinetic model described in this paper. Typically, the reaction should be stirred at least 6 h to ensure complete conversion of KOCN.
(43) See Supporting Information for HPLC and UPLC purity methods, including retention times and relative response factors for individual components.
(44) EtOAc was added to scavenge any hydroxide in order to prevent ester hydrolysis during the reaction.
(45) Some of the NaOEt was consumed by dehydrobromination of the alkylating agent.
(46) The $NaHCO_3$ typically removes 1.5−2% residual **4**, 1.5−2% of diacid **10**, and 3−5% **5**. Using a slight excess eliminates the need for an in-process assay.
(47) Samples were quenched into MeOH containing 1% pyridine (v/v) and analyzed by the UPLC purity method. See the Supporting Information for method conditions.

The resulting acid chloride solution was added to a slurry of semicarbazide **16** (2.64 kg, 98.4% assay, 14.49 mol, 1.0 equiv) in pyridine (1.51 kg, 19.1 mol, 1.30 equiv) and toluene (34 L) over 0.5 h while maintaining the temperature below 40 °C. The lines were rinsed with toluene (4 L) and the reaction was stirred at 25 °C until the reaction was complete (at least 1 h).[48]

(±)-**10**-Camphorsulfonic acid (6.83 kg, 29.40 mol, 2.00 equiv) was added, and the reaction mixture was heated to 100 °C and stirred for 3 h. The reaction mixture was cooled to 80 °C, and a 2.5 M of H_2SO_4 in EtOH (7.57 kg of 2.5 M solution, 19.7 mol, 1.34 equiv)[49] was added over 10−15 min. **Caution!** Care should be exercised in handling this solution, which is corrosive and contains significant levels of $EtOSO_3H$.[28,29] The reaction was heated at reflux (∼80 °C) for about 2 h, until **25** has decreased to <0.5% by area relative to triazolone **8**. After cooling to room temperature, the reaction mixture was transferred over 0.5 h into a solution of $NaHCO_3$ (6.55 kg, 78.0 mol) in H_2O (27 L) at a rate to control gas evolution and to maintain the pH in the quench mixture above 5.5. The phases were separated and the organic phase was washed with H_2O (27 L). After phase separation, the organic phase was concentrated to ∼13 L (3 volumes) by vacuum distillation 36−52 °C/100−150 mmHg. After the addition of heptane (5.5 L, 3.76 kg), the crystallization was seeded with **8** (0.34 kg, 0.77 mol, 0.052 equiv) at 37 °C, and the mixture was stirred for 10 min. Heptane (12.59 kg, 18.4 L) was added slowly over 2.5 h with stirring, while maintaining the temperature at 37 °C. When the addition was complete, the slurry was cooled with stirring to 10 °C over 3 h with a cooling rate of ∼8 °C/h and was stirred for an additional 1 h. The solid was filtered and was washed, with stirring, with a 10 °C solution of 3:1 *n*-heptane (15 L)/toluene (5 L). This was followed by two cake washes (16 L each), without stirring, with a 10 °C solution of 3:1 *n*-heptane/toluene. Triazolone ester **8** (4.405 kg, 99.27% assay, 99.69% purity, 63.6% yield) was obtained as a white crystalline solid after vacuum drying for approximately 15 h at 50 °C/100 mmHg, mp 95.5−97.1 °C. Anal. Calcd for $C_{25}H_{31}N_3O_4$: C, 68.63; H, 7.14; N, 9.60; O, 14.63. Found: C, 68.43; H, 7.14; N, 9.57. ^{1}H NMR (DMSO-d_6: δ 1.14 (t, J = 7.1 Hz, 3H), 1.47 (s, 6H), 1.79 (quintet, J = 7.6 Hz, 2H), 2.24 (s, 3H), 2.34 (m, 2H), 2.48 (m, 2H), 4.13 (q, J = 7.1 Hz, 2H), 4.70 (s, 2H), 6.67−6.70 (m, 2H), 7.02−7.05 (m, 2H), 7.08−7.12 (m, 4H), 11.41 (s, 1H, D_2O exch). ^{13}C NMR (DMSO-d_6: δ 14.3, 21.1, 25.5 (2C), 26.0, 28.1, 33.8, 47.48, 61.4, 79.0, 119.3 (2C), 127.9 (2C), 129.4 (2C), 129.5 (2C), 135.0, 135.3, 136.9, 146.4, 153.6, 154.7, 173.7. IR (KBr): 3436, 3097, 2990, 2921, 1726, 1698, 1611, 1510, 814, 756, 740, 722 cm^{-1}. HRMS (m/z, M + 1): Calcd for $C_{25}H_{32}N_3O_4$: 438.2387. Found: 438.2377.

2-[4-[3-[2,5-Dihydro-1-[(4-methylphenyl)methyl]-5-oxo-1H-1,2,4-triazol-3-yl]propyl]phenoxy]-2-methylpropanoic Acid (LY518674, 1). *Caution!* PPARα agonist LY518674 (**1**) and its ester derivative **8** are highly potent compounds[5,8] and should be handled with extreme caution to prevent worker exposure.

Sodium hydroxide (25.7 kg of 1 N NaOH, 25 mol, 2.19 equiv) was added to **8** (4.99 kg, 11.40 mol, 1.0 equiv). The resulting pale-yellow solution was stirred at 25 °C for 6 h until <0.1% of **8** remained by HPLC. Ethyl acetate (60 L) was added, and the resulting mixture was stirred for at least 3 h (pH 9.97 at end of stir time). The pH was adjusted to 1.75 by addition of 5 N HCl (5.30 kg, 24.7 mol, 0.99 equiv). The organic phase was washed with H_2O containing 2% EtOH by weight (20 kg H_2O + 0.4 kg EtOH).[33] The organic phase was polish filtered through a 20 μm cartridge filter, and the line was rinsed with EtOAc (2 L). The filtered solution was concentrated to about 12 L (2.3 volumes) by vacuum distillation at 70−80 °C/740 mmHg. Additional EtOAc (25 L) was added, and the distillation was continued to the same end point. After additional EtOAc (48 L) was added and the temperature was adjusted to 60 °C, the solution was seeded with **1** (0.050 kg, 0.12 mol, 0.01 equiv). The mixture was stirred at 60 °C for 1 h before cooling to 5 °C at a rate of 0.2 °C/min over 4.6 h. The slurry was filtered after stirring for 1 h. The cake was washed with two portions of 5 °C EtOAc (15 L each), the first with stirring of the slurry, and the second without stirring. PPARα agonist **1** (4.49 kg, 99.6% assay, 99.85% purity, 96% yield) was obtained as a white powder after vacuum drying for approximately 18 h at 60 °C/100 mmHg, mp 130.7−131.2 °C. Anal. Calcd for $C_{23}H_{27}N_3O_4$: C, 67.46; H, 6.65; N, 10.26; O, 15.63. Found: C, 67.55; H, 6.75; N, 10.29. ^{1}H NMR (DMSO-d_6: δ 1.48 (s, 6H), 1.82 (m, 2H), 2.27 (s, 3H), 2.38 (m, 3H), 2.50 (m, 2H), 4.74 (s, 2H), 6.76 (m, 2H), 7.07 (m, 2H), 7.14 (s, 4H), 11.46 (s, 1H, D_2O exch), 12.99 (s, 1H, D_2O exch). ^{13}C NMR (DMSO-d_6: δ 21.1, 25.5 (2C), 26.0, 28.2, 33.8, 47.5, 78.7, 119.0 (2C), 127.9 (2C), 129.4 (2C), 129.5 (2C), 134.9, 135.0, 136.9, 146.4, 153.9, 154.73, 175.6. IR (KBr): 3085, 3033, 3013, 2994, 2949, 2930, 3500, 2500, 1731, 1683, 1611, 1589, 1507, 1472, 1437, 1264, 1232, 1180, 1147, 833, 808, 642 cm^{-1}. UV (MeOH): 205 nm (ε 21690), 220 nm (ε 19819), 275 nm (ε 891). HRMS (m/z, M − 1): Calcd for $C_{23}H_{26}N_3O_4$: 408.1929. Found: 408.1927.

CCDC 702044-702048 contains the supplementary crystallographic data for this paper, which includes data for compounds: **1**, **5**, **8**, **16**, and **17**. These data can be obtained free of charge via http://www.ccdc.cam.ac.uk/cgi-bin/catreq.cgi, by emailing data_request@ccdc.cam.ac.uk, or by contacting The Cambridge Crystallographic Data Centre, 12, Union Road, Cambridge CB2 1EZ, U.K.; Fax: +44 1223 336033.

Acknowledgment

The development and scaleup of a multistep process involves a large number of talented scientists and technical personnel. We express our gratitude to the following individuals: Matthew Allgeier, Dr. Todd Gillespie, Maryam Mostafavi, Jean-Claude Garay, Dr. Thomas Zennie, and Lisa Zollars for providing analytical support and assistance with the characterization of API impurities; Dr. P. Y. Chen, Michael Heller, John Howell, Jeffrey Lewis, Robert Metzler, Richard Miller, Gary Richardson, Otis Williams, and the API Operations staff for their technical assistance in process scaleup; Robert Waggoner for handling all procurement activities for the program; Amanda McDaniel for assistance with the kinetic modeling studies; Jeff Bieszki and John Simms of Waters Corporation for their technical

(48) Analytical data for compound **7** is included in the Supporting Information.

(49) A stock solution was prepared by the slow addition of 98% H_2SO_4 (6.51 kg, 65.0 mol) to absolute 2B-3 EtOH (23 L, 394 mol) and stored at room temperature.

assistance with the Waters ACQUITY UPLC system; Dr. Gregory Stephenson for X-ray crystal structure analysis; and Dr. Alain Merschaert for his helpful technical discussions. Finally, we thank the management team of Chemical Product Research and Development at Eli Lilly and Company for providing the state-of-the-art development research equipment used on this project.

Supporting Information Available

(1) Outline for using an export method for rapid reaction profile generation; (2) additional details related to development of the kinetic model for reaction of KOCN with hydrazine **15**; (3) comparison of the reaction profiles using pyridine and DMF as catalysts for acid chloride formation; (4) the fractional factorial design used for process optimization leading to **6**; (5) HPLC and UPLC analytical methods and relative response factors for several components; (6) solubility data used during crystallization development for triazolone **8**; (7) spectral characterization and experimental procedures for the synthesis of the following compounds: API impurities (**9**−**14**) and their synthetic precursors, nonisolated intermediate **7**, and **17**−**22**, **24**, **25**, **27**, and **28**. This material is available free of charge via the Internet at http://pubs.acs.org.

Received for review September 30, 2008.

OP8002486